Drying of cable backfill by vapour diffusion balanced by capillary water suction: a laboratory experiment with altered groundwater levels

Case Studies in Thermal Engineering 47 (2023) 102941

Contents lists available at ScienceDirect

Case Studies in Thermal Engineering

journal homepage: www.elsevier.com/locate/csite

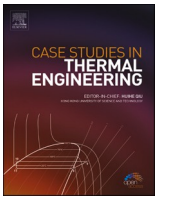

Drying of cable backfill by vapour diffusion balanced by capillary water suction: a laboratory experiment with altered groundwater levels

H.P. Lidén *, B. Adl-Zarrabi, J. Sundberg

Dept. of Architecture and Civil Engineering, Chalmers Univ. of Technology, Sven Hultins gata 8, Göteborg, SE- 412 96, Sweden

ARTICLE INFO

Handling Editor: Huihe Qiu

Index Terms:
Cable sand
dry out
Heat transfer
HVDC
Groundwater level
Vapour diffusion
Capillarity

ABSTRACT

The performance of underground infrastructures, such as an electrical transmission cable, is strongly affected by transmission-induced high temperatures, which have an impact on the properties of the cable and the electric load. Therefore, it is essential to determine if a high load will cause a dry out of a sandy thermal backfill close to the cable. This paper aims at describing processes and establishing criteria for when a dry out can occur. Processes that are addressed are e.g., vapour diffusion and capillary water transport. Criteria of interest are e.g., groundwater levels and capillarity of soil. A new pilot laboratory experiment, with varying groundwater levels, was developed to investigate the dry out of the cable sand in close proximity to an operating cable. The experimental results show that a thermal backfill can withstand a dry out, at a high current load in a cable, if there is a capillary contact to a groundwater level 2 m below the backfill material.

Symbols

T	Temperature (K)
ρc	Volumetric heat capacity (J/m^{3}K)
$\dot{q}$	Heat source (W/m^3)
Q	Heat loss (W)
λ	Thermal conductivity (W/mK)
$Ø$	Diameter (mm)
t	Time (s)
d_{50}	Medium value of grain size distribution (mm)
m	Mass (kg)
ρ	Density (kg/m^3)
C_p	Specific heat capacity (J/Kg/K)
V	Volume (m^3)
A	Surface area (m^2)
Ke	Kersten number (−)

* Corresponding author.
E-mail address: Peter.Liden@ri.se (H.P. Lidén).

https://doi.org/10.1016/j.csite.2023.102941
Received 18 January 2022; Received in revised form 16 March 2023; Accepted 23 March 2023
Available online 7 April 2023

h	Heat transfer coefficient at external surfaces (W/m^{2}K)

Subscripts

app	apparent
ac	after compaction
as	after saturation
as	after saturation
ee	end of experiment
c	convection
s	surface
w	water
dry	dried at 105 °C
a	air
sat	saturated

Acronyms

HVDC	High Voltage Direct Current
H	cable sand Hamneda
SS	cable sand Södra Sandby
GWC	Gravimetric Water Content (Kg/kg)
VWC	Volumetric Water Content (m^3/m^3)

1. Introduction

Underground high voltage direct current (HVDC) cables have the advantage of taking up less surface space. They are also less affected by surface climate conditions than traditional overhead transmission lines, which also have a negative esthetical impact [1]. In an operational HVDC cable, heat is generated due to the electric resistance of the conductor, a resistance that increases with increasing temperatures. The current-carrying capacity (the ampacity) of a cable system is influenced by the ability of the installation to dissipate the heat from the cable, into the surrounding medium [2,3]. The maximum operating temperature of the conductor varies between 55 and 90 °C among different cable types [4], where a conductor temperature of 90 °C approximately leads to a cable surface temperature of 70 °C [5]. A cable is designed for an ampacity that generates a certain maximum temperature, related to the lowest allowed thermal conductivity (λ) of the thermal backfill (cable sand), which is surrounding the cable. Thus, a highly conductive backfill environment would allow for higher ampacity. However, if the design temperature is exceeded, it may influence the warranty from the manufacturer [1]. The functionality and lifetime of the cable can, in extreme cases, lead to a thermal runaway, and breakdown of the cable [1,6].

Thermal energy can be transported in soil by heat conduction, radiation, and convection. Radiation generally has minor influence [7] but can be of importance in e.g., very coarse material with low water content at elevated temperature. At higher temperatures, heat can also be transferred by diffusion of water in both the gas and liquid phase. In addition, advective heat transport can also take place by forced convection e.g., groundwater flow driven by hydraulic gradients [8]. Above the groundwater level, and at normal ground temperatures, heat conduction is the governing transport mechanism. The heat flow is linearly dependent on λ. High water content, high density of soil, and high quartz content are the most important factors to obtain high λ at normal temperatures. To determine λ of a material at elevated temperature or experimentally in the field, it is appropriate to use apparent thermal conductivity (λ_{app}), since other heat transfer mechanisms may contribute to the result. At higher temperatures and intermediate degrees of saturation, vapour diffusion contributes to raising λ_{app} and increasing the heat transfer.

Near the cable surface, evaporation of water takes place and vapour is transported in the direction of the heat flow. This is illustrated in Fig. 1, where vapour migration induces a lower water content near the cable, which in turn induces a capillary water suction in the opposite direction, towards the cable. However, if the suction of liquid water for some reason cannot balance the vapour diffusion, the water content decreases, which leads to a decrease in λ_{app} and elevated temperature.

The heat flow, induced by the cable, is the main driving force for all other mechanisms. A low cable temperature gives less influence

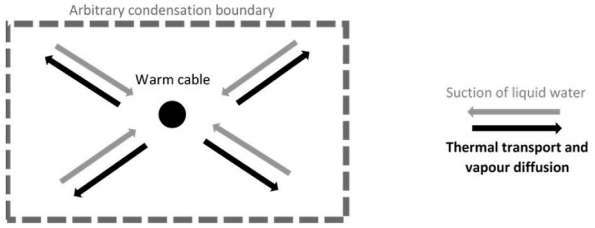

Fig. 1. Simplified systematic sketch for coupled heat and moisture transport in the soil surrounding an operating cable.

on the vapour diffusion. A high λ_{app} gives lower temperature, and thermal gradient under steady-state conditions and less tendency for the soil to dry out. Grain size distribution of the cable sand highly affects the water retention capacity, especially the amount of fine-grained material, which controls the water content in the soil in general and close to the cable in particular. A soil with a high water retention capacity is less prone to dry out.

Experimental and numerical studies have earlier been performed to quantify heat dissipation from underground cables, and in some cases also to predict when the close surroundings of the cable may dry out [9–14]. Different types of backfill material are well studied, also the beneficial effects from using artificial backfill materials. In some cases, the moisture content was also controlled by regulating the matric suction in the sample [9,10,15,16]. That approach helps to systematically study the role of moisture content between samples with equal density. Previous studies are thorough and show the development of a dry out with constant loading, as well as under cyclic loading [13,17,18]. However, the experimental setups did not appear to allow for suction of liquid water for balancing moisture migration. Thereby, a dry out is the predetermined outcome.

The present paper presents a laboratory experiment in which the physical processes around an operating cable are investigated. In contrast to prior work, the proposed experimental setup allows for the liquid water suction to take place by capillarity, and thus mimic real conditions in the field. In addition, suction is also locally measured rather than controlled. Furthermore, a finite element model is developed for detailed interpretation of the experiment, such as the effect of high temperature and low water content on the apparent thermal conductivity.

2. Experimental methodology

2.1. Test setup

In the present experimental setup, a steel sample holder with a height of 180 mm and diameter of 320 mm was equipped with an electrical heating rod Ø8 x 320 mm (with a built-in thermocouple) in the center of the sample holder, a ceramic plate with a thickness of 10 mm, a tensiometer Ø23 mm and type-K thermocouple sensors, range 0 °C to + 400 °C, accuracy ± 0.4 °C, diameter 0.2 mm. The sample holder was insulated by a 70 mm thick insulation material of mineral wool, except for the bottom of the sample holder, where 20 mm insulation of cellular plastic was placed. The sample holder was connected to a vacuum pump, for control of the groundwater level, see Fig. 2.

Two cable sand materials were used in this experiment, Södra Sandby (SS) with grain size 0–5 mm, d_{50} 0.5 mm and dry density 1976 kg/m^3 and Hamneda (H) with grain size 0–4 mm, d_{50} 0.45 mm, and dry density close to 1800 kg/m^3. The cable sand was placed in the sample holder, connected to vacuum containers. The heater mimicked a cable in operation. The groundwater level was controlled by suction in the ceramic plate. The suction in the cable sand was measured by a tensiometer 5 mm from the heating rod, see Fig. 2. The temperature close to the heating rod was measured in three points by thermocouples type K, spaced horizontally 5, 10, and 20 mm from the center of the horizontal heating rod, but with 10 mm offset from each other and vertically in line with the heater. Furthermore, temperatures for the steel side, steel lid of the sample holder, and ambient temperature were also measured and sampled with the logger, dataTaker DT85.

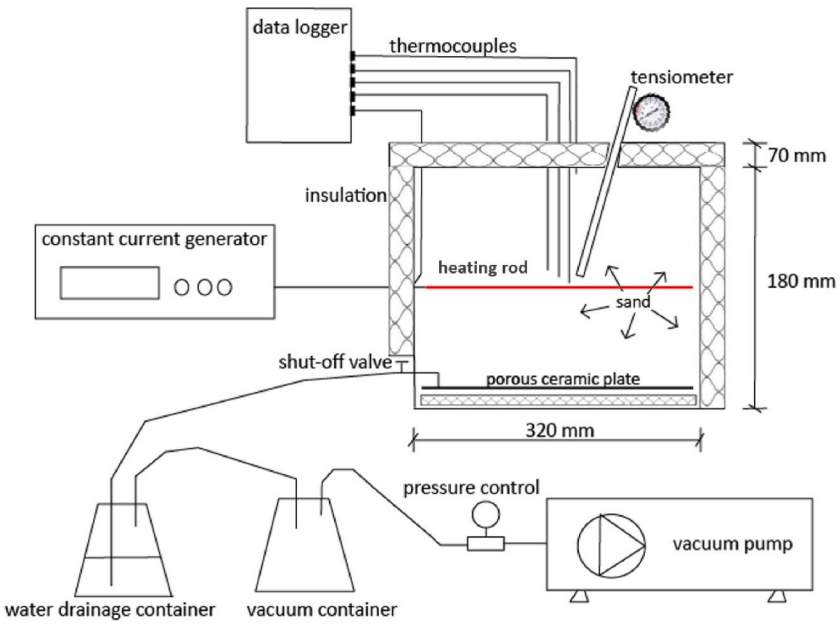

Fig. 2. Experiment setup.

2.2. Measurement procedure and results

The sand material in the sample holder was compacted according to standard proctor compaction. Thereafter, the samples were saturated with tap water from the bottom and up for one night (12 h). The required power in the heating rod was unknown. Thus, the temperature of the heating rod was stepwise raised by electrical power with a constant resistor, up to the desired temperature level of approximately 75 °C. In the next step, the "ground" water level was decreased by using the vacuum pump, and stepwise increasing the suction to −5 kPa, −10 kPa, −20 kPa, and −40 kPa, which correspond to groundwater levels of −0,5 m, -1m, -2m and -4m below the heating rod. Groundwater levels vary with climate conditions and topological conditions, mainly in recharge areas. However, there is a low variation of the groundwater level in discharge areas, with levels close to the ground surface [19]. The groundwater levels in this experiment were selected based on typical groundwater levels in Swedish moraines and sandy soils, which are 1–4 m below soil surface [20]. Finally, the water in the cable sand was first fully drained and then oven-dried at 105 °C, to establish the total dry condition.

Density, gravimetric and volumetric water content were measured after compaction, saturation, and at the end of the experiment, see Table 1. The sands fall within the range of typical coarse-grained backfill materials. The λ of the material was measured at three occasions by using the thermal needle probe method, which follows ASTM standard D5334-14 [21]: first after compaction (ac) of the cable sand material in the sample holders, then after water saturation (as) and finally at end of the experiment (ee). The results are presented in Table 1.

The most significant difference between the cable sands was the mineral content. For cable sand SS, there was a much larger content of the highly conductive mineral quartz compared to cable sand H, which resulted in a higher λ. The larger proportion of smaller grain size in cable sand H, allowed for a higher capillarity and water retention capacity compared to cable sand SS. Especially at intermediate volumetric water content. The negative matric potential on the y-axis in Fig. 3, symbolizes the groundwater level (m) below a cable. The lowest points correspond to λ at the saturated state, and the highest points correspond to λ at the end of the experiment.

3. Numerical modelling

A numerical model was developed in COMSOL Multiphysics for the evaluation of heat and moisture transfer in the experimental setup. The partial differential equation for heat transfer was solved in 3D, by using Eq. (1). Convective heat transfer boundary conditions have been used for all external surfaces of the sample holder, calculated by using Eq. (2). The heat transfer coefficient was calculated to 5 W/(m^2•K). In the numerical model, the thermal conductivity of the cable sand is a function of temperature. Furthermore, the influence of water content and vapour diffusion on the temperature field, were treated by using a calculated λ_{app}, see chapter 3.1.

$$\rho C_p \frac{\partial T}{\partial t} = \lambda_{app} \nabla^2 T + \dot{q} \tag{1}$$

$$Q_c = h_c A (T_s - T_a) \tag{2}$$

In Eq. (1) ρ is density (kg/m^3), C_p is specific heat capacity (J/Kg/K), $T = T(x, y, z, t)$ is temperature as a function of space and time, λ_{app} is apparent thermal conductivity (W/(mK)) and $\dot{q}$ is a heat source (W/m^3). In Eq. (2) Q_c is heat loss from sample holder (W), h_c is heat transfer coefficient at external surfaces outside the insulation, $h_c = 2\left|T_s - T_a\right|^{1/4}$ (W/(m^{2}K)), A is surface area (m^2), T_s is the surface temperature (K) and T_a is air temperature (K).

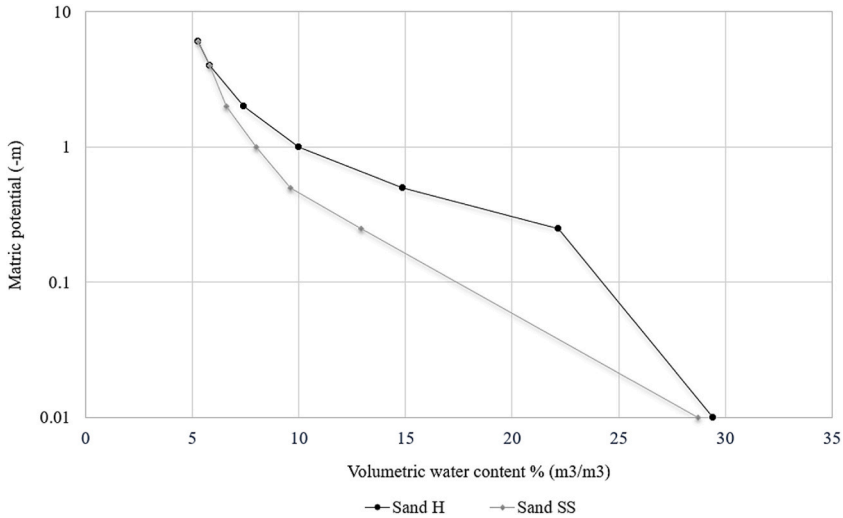

Fig. 3. Water retention curves.

3.1. Calculation of apparent thermal conductivity in the model

The heat transfer in partially saturated cable sand at high temperatures is very complex to model. The uncertainties are high, which some of the previous models show [22–26]. The influence of temperature and water content on λ_{app} were calculated using the empirical relations Eqs. (3) and (4), which were proposed by Tarnawski, Leong [27]. λ_{dry} and λ_{sat} are known, see Table 1, where λ_{dry} corresponds to λ_{ee}. The temperature-dependent equations, which were chosen for their simplicity, are based on Eq. (3) by Johansen [28], which includes the Kersten function *Ke* [29]

$$\lambda_{app} = \lambda_{dry} + \left(\lambda_{sat} - \lambda_{dry}\right) Ke \tag{3}$$

$$Ke = \frac{\mathrm{a} + \mathrm{bT} + \mathrm{cS_r} + dS_r^2}{1 + \mathrm{eT} + \mathrm{fS_r} + \mathrm{g}S_r^2} \tag{4}$$

where *Ke* is the modified Kersten number, and *T* is the temperature. The fitting coefficients shown in Table 2 derive from soils categorized 'coarse' in Tarnawski et al. (2000). This is a soil type similar to the cable sands in this lab experiment.

The calculated impact from temperature and volumetric water content, on the apparent thermal conductivity in cable sands SS and H, is presented in Fig. 4 and Fig. 5 respectively.

Figs. 4 and 5 show the variation of λ_{app} of cable sand as a function of moisture content and temperature, by using Eqs. (3) and (4). At the total dry state, vapour diffusion is zero and does not affect λ_{app}, likewise for the saturated state. The calculated results presented in Figs. 4 and 5 indicate that the influence of temperature variation on λ_{app} is significant when the volumetric water content is between 10% and 15%. For this span, for both cable sand SS and cable sand H, λ_{app} increases with 60–70% with a temperature increase from 30 to 90 °C.

3.2. Boundary condition in the model

The model was calibrated with respect to its outer boundary. Heat dissipation varied from the sample holder due to variations in the insulation, and due to the perforating tensiometer. For this reason, the model was calibrated by the temperature measurement results, at the heating rod as well as 5 mm and 20 mm from the heating rod, by increasing the thermal conductivity of the insulation.

Fig. 6 and Fig. 7 show a comparison between calculated temperatures by the calibrated model and the temperatures measured by the suggested setup for the two different sand types, SS and H. The calibration is based on the maximum deviation between measured and calculated temperatures, in the range 37°C–57 °C. For cable sand SS there is a small difference between measured and calculated temperatures for all compared points. The difference in heater temperature for measured and calculated temperature was 0.25 °C.

In the numerical calculations, cable sand H, in comparison to cable sand SS, has a larger but acceptable difference between measured and calibrated temperatures for all compared points. Less than 5%. The difference in heater temperature for measured and calculated temperature was approximately 1 °C. For cable sand H, it seems like the thermocouples have been dislocated a few millimeters away from the heater during the installation, and due to compaction of the cable sand.

4. Results and discussion

Results of temperature measurements obtained by the laboratory tests, which are compared to numerically calculated temperatures, are presented in Fig. 8 and Fig. 9, for cable sand SS, and cable sand H respectively. The measured temperatures are displayed for each cable sand, with the heating rod during the experiment (solid red in Figs. 8 and 9) as well as calculated temperatures for three different thermal conductivities (dashed lines in Figs. 8 and 9). The room temperature (solid grey) had an impact on the sample temperatures, therefore included in the figures.

For the calculated temperatures, two constant thermal conductivity levels and one thermal conductivity varying by temperature and moisture content were used. The constant thermal conductivities for cable sand SS, λ_{ac} and λ_{ee}, were 2.15 W/mK and 1.96 W/mK respectively, and for cable sand H, λ_{ac} and λ_{ee} were 1.64 W/mK and 1.11 W/mK respectively. The variable thermal conductivities λ_{app} were in the range of 1.92–3.85 W/mK for sand SS and 1.12–2.43 W/mK for sand H.

From the start of the experiment until approximately 1500 h, the difference in the calculated temperatures between constant and variable conductivities increases. This is shown by a comparison between the calculated temperature (λ_{app}), and the calculated temperature by the constant conductivities, see Figs. 8 and 9. The increase is most distinguishable for cable sand H. This deviation is

Table 1
Measured properties for cable sands H and SS at room temperature.

Sand	Status[a)]	Density kg/m^3	Dry density kg/m^3	GWC[b)] m_w/m_{dry}	VWV[b)] V_w/V_{tot}	λ W/(mK)
H	ac	1896	1801	0.050	0.090	1.64
	as	2019	1801	0.118	0.292	1.79
	ee	1869	1822	0.025	0.046	1.11
SS	ac	2080	1976	0.050	0.099	2.15
	as	2187	1976	0.105	0.287	3.14
	ee	2111	2058	0.026	0.054	1.96

[a] ac: after compaction as: after saturation ee: end of experiment.
[b] GWC: Gravimetric water content VWC: Volumetric water content.

Table 2
Fitting coefficients [27].

Coefficient	a	b	c	d	e	f	g	S^2r
value	0.128	- 0.0012	0.556	1.167	−0.0074	−0.841	2.099	0.932

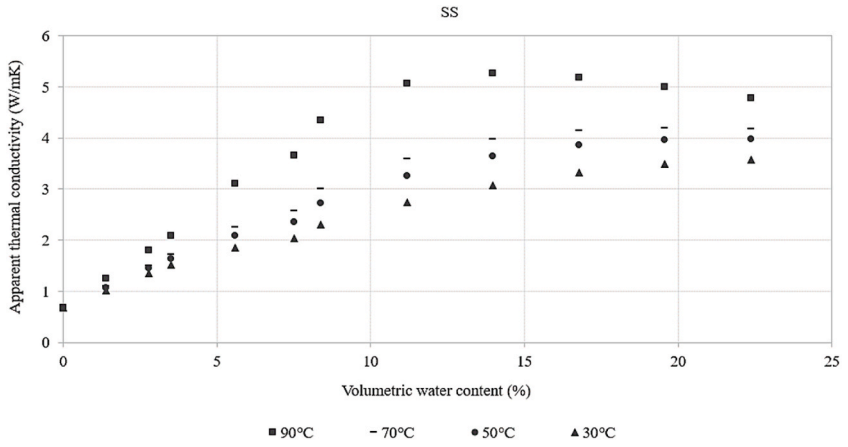

Fig. 4. Calculated λ_{app} by Eqs. (3) and (4) versus volumetric water content in temperature span 30–90 °C for cable sand SS.

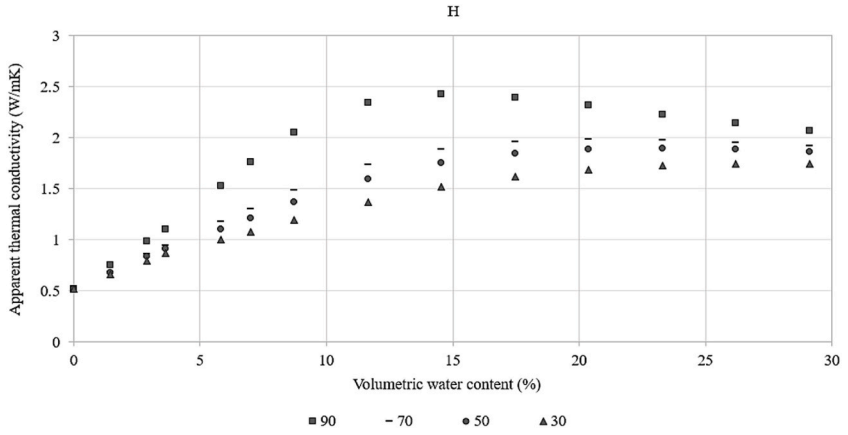

Fig. 5. Calculated λ_{app} by Eqs. (3) and (4) versus volumetric water content in temperature span 30–90 °C for cable sand H.

more significant after about 500 h and 55 °C. This mean that up to this level of temperature, the influence of varying thermal conductivity by temperature and moisture content is low. After about 500 h, when the difference increases furthermore, it coincides more with the experimental results from the guarded hot-plate method by Nikolaev et al. [26], i.e. a high thermal conductivity in partially saturated cable sand at high temperatures. However, the increasing level in λ_{app}, seems to be smaller than what was found by Nikolaev et al. [26].

The calculated temperatures with the λ_{app}, had a better match to heater temperature measurements of cable sand SS than to cable sand H, in the temperature range 20–55 °C. However, above 55 °C the calculated temperatures with the λ_{app} had a better match for cable sand H than for cable sand SS. Further research is needed to clarify the reason of this mismatch of the results, regarding certain temperature ranges and sands.

The small scale of the experiment partly affected the hypothesis of establishing a system that represents the conditions for an operative cable in a real underground installation, at shallow depth. The hypothesis relied on that the vapour condensates within the cable sand further away from the heat source, and liquid water then flows back towards the heater by capillary suction. The hypothesis of balanced vapour diffusion, and suction of water was confirmed, but in a different way than expected. Condensation did not happen due to the small scale of the experimental setup, and because water vapour diffused out through the sample holder in the opening for the tensiometer. Instead of condensation, water was transported upward from the water drainage container. Furthermore, the tensiometer had higher suction closer to the heat source in the sample holder than the created vacuum by the vacuum pump, see Fig. 10. This indicates that a water transport took place from the lower levels of the sample holder to the level of the heating rod.

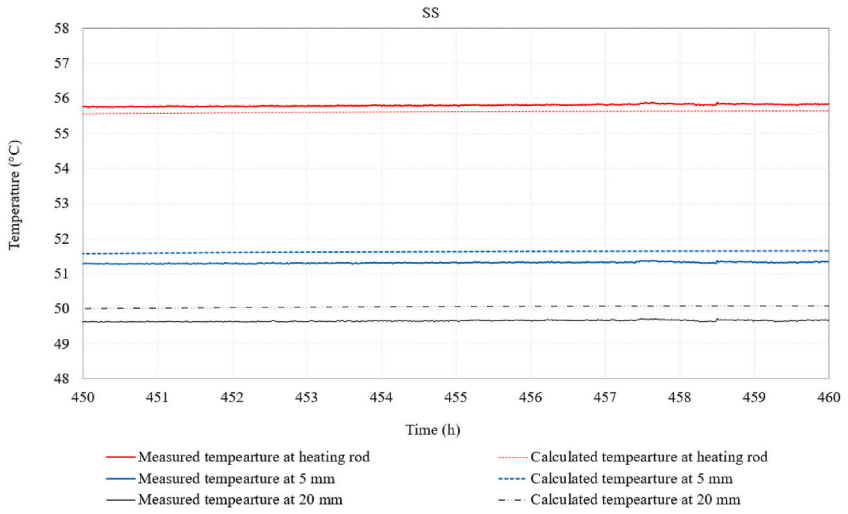

Fig. 6. Cable sand SS, comparison between measured and calculated temperatures in the temperature interval 48–58 °C.

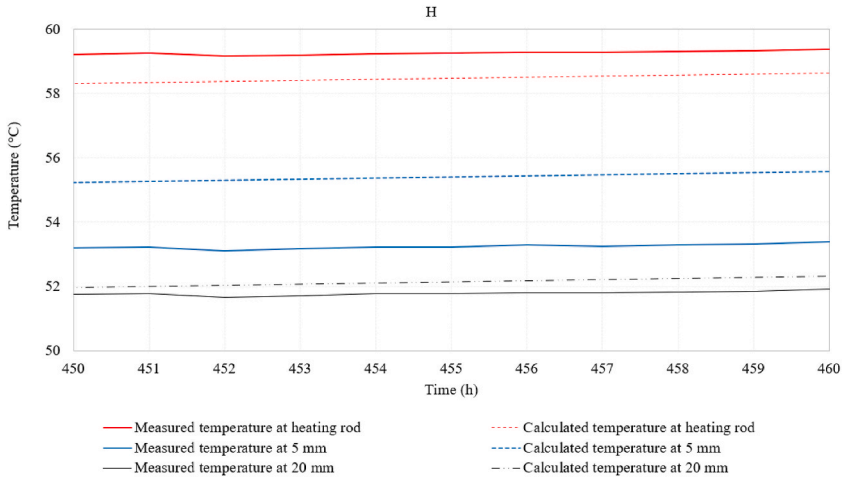

Fig. 7. Cable sand H, comparison between measured and calculated temperatures in the temperature interval 50–60 °C.

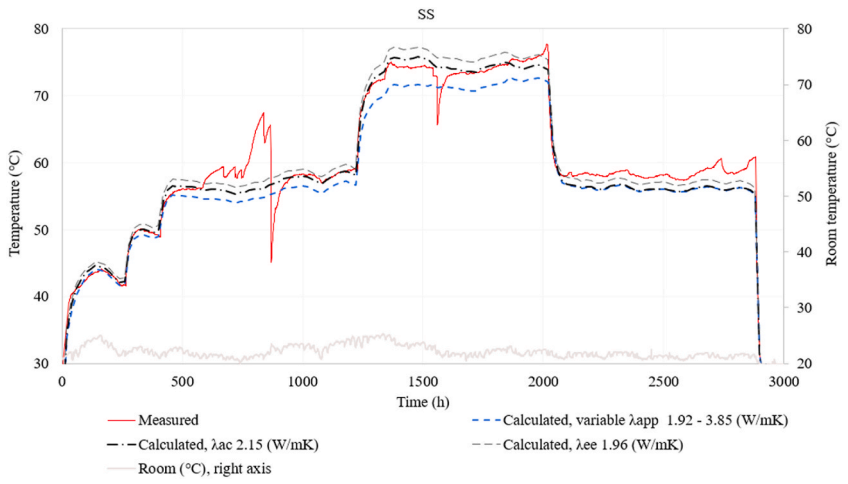

Fig. 8. Measured and calculated temperatures of heating rod for cable sand SS for 2900 h.

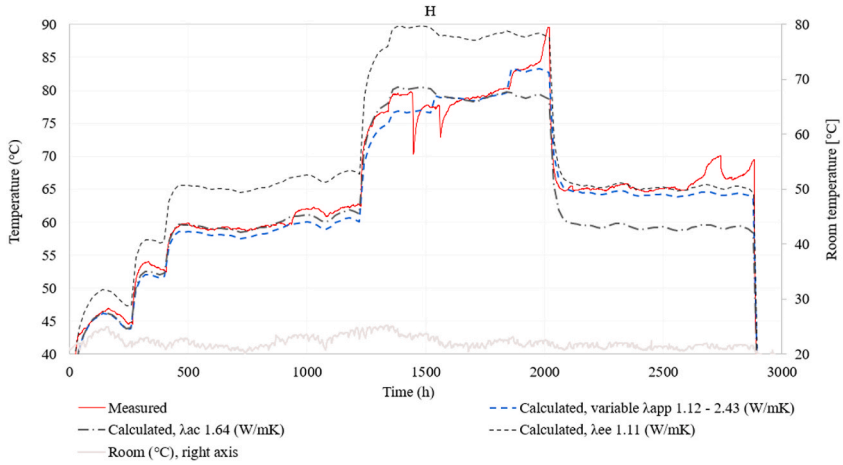

Fig. 9. Measured and calculated temperatures of heating rod for cable sand H for 2900 h.

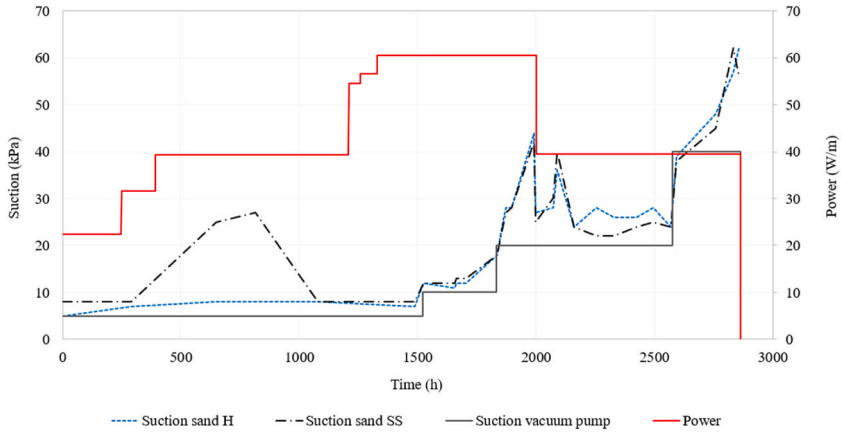

Fig. 10. Suction in cable sands H and SS from tensiometer (kPa), suction from vacuum pump (kPa), and power to the heating rod (W/m).

During the experiment, potential dry outs occurred close to the heater, only when the capillary water contact was broken. In Fig. 9 these are shown as peaks (when vacuum suction is unchanged). The broken contact, which also was visible in a transparent drainage tube, always caused fast raising temperatures in the following days. On these occasions, the heating rod was temporarily disconnected for safety reasons, which are shown by the rapid temperature drops in Figs. 8 and 9 (at 860 h and 1560 h for cable sand SS and 1425 h and 1545 h for cable sand H). The broken capillary contact may have been caused by leakage of air into the shut-off valve connections, especially when higher suctions were created with the vacuum pump. Broken water contact might also have occurred due to dehydration of the ceramic plate, caused by too high temperatures because of the insufficient distance between the heating rod and the ceramic plate.

Fig. 10 also shows the total heat flow from the heating rod in the experiment, with a range from 22.4 to 60.5 W/m, which is about 2–3 times larger than during real underground conditions of a HVDC cable. This is more than 30 times higher when measured in W/m^2, therefore a highly conservative condition. The experiment showed that even if the heating rod generated a high heat flow and high temperatures, no drying out occurred as long as there was a constant water flow towards the cable. In Fig. 10 this is shown from experimental start until 1500 h, where the suction in cable sand H was stable, even though the power reached its highest levels. First, when there was a change in vacuum suction, the cable sand responded with higher suction. The largest suction that could be created during a long period with this experimental setup, without any dry outs, was 20 kPa (groundwater level 2 m below the heating rod). This period is shown in Figs. 8–10, between 2100 h–2500 h. For this period, a suction of 25 kPa in the sands corresponds to a matric potential of −2.5 m. This indicates a volumetric water content of approximately 7–8%, see the water retention curve in Fig. 3. It is unclear when the magnitude of the heat flow and the temperature, becomes more dominant than the ability of the liquid water to flow back due to the difference in suction. This cannot be illustrated in the experiment, since the observed dry outs occurred after a broken capillary connection.

5. Conclusions

In the vicinity of an operating cable in sandy backfill material, there are complex physical processes taking place, and backfill design plays a major role. The design can be conducted in a conservative manner, meaning calculating maximum cable conductor temperature, with surrounding backfill material in a dry state. This is a worst-case scenario, which prevents a thermal runaway and breakdown of cable insulation. However, this paper indicates that a less conservative approach may be used with knowledge of the groundwater levels, and the soil material underlaying the cable bed. A less conservative approach may be taken for cable routes passing groundwater discharge areas, due to the lower variation in groundwater levels.

It can be concluded by the experimental results that:

- A high heat transport could be maintained from the cable if there was a capillary contact between the cable sand and the groundwater level.
- Avoiding high temperature close to the cable was possible, especially for cable sand SS, which contained the highly conductive mineral quartz.
- Stable temperatures were maintained for 400 h for both cable sands, even though the electrical load was 2–3 times higher than typical design values, measured in W/m, and more than 30 times higher when measured in W/m^2. These temperatures remained stable even though the groundwater level was 2 m below the cable.
- The numerical model could illustrate that high temperatures and low water content contributed to a higher apparent thermal conductivity in the cable sand. Thus, it may be possible to account for increased heat transfer, which then would allow for a higher ampacity in the cable, without exceeding design temperature.

The desired condition, with no thermal runaway, is expected to be fulfilled when the following criteria are taken into consideration in the backfill design: proper compaction and high water retention capacity of the cable sand material, and high enough capillarity of the natural soil material down to the groundwater level.

For further research, the experimental setup can be improved by upscaling, to allow for a larger temperature gradient within the sample, and to make room for condensation to take place in the cable sand. Moreover, additional soil types could be evaluated.

Author statement

We hereby declare that we are the authors of this manuscript.

Declaration of competing interest

The authors declare that they have no known competing financial interests or personal relationships that could have appeared to influence the work reported in this paper.

Data availability

Data will be made available on request.

References

[1] J. Sundberg, Evaluation of Thermal Transfer Processes and Back -fill Material Around Buried High Voltage Power Cables. 2015, Department of Civil and Environmental Engineering, Division of GeoEngineering, vol. 5, Chalmers University of Technology, 2016.
[2] M. Rerak, P. Ocłoń, The effect of soil and cable backfill thermal conductivity on the temperature distribution in underground cable system, E3S Web Conf. 13 (2017), 02004.
[3] G. Plumettaz, J. Heinonen, High voltage energy cables go underground – how to improve installation efficiency, in: Nternational Wire & Cable Symposium, 2010.
[4] G. Chen, et al., Review of high voltage direct current cables, CSEE J. Power Energy Syst. 1 (2) (2015) 9–21.
[5] C.J. Emeana, et al., The thermal regime around buried submarine high-voltage cables, Geophys. J. Int. 206 (2) (2016) 1051–1064.
[6] C.C. Reddy, T.S. Ramu, On the computation of electric field and temperature distribution in HVDC cable insulation, IEEE Trans. Dielectr. Electr. Insul. 13 (6) (2006) 1236–1244.
[7] J.K. Mitchell, K. Soga, Fundamentals of Soil Behavior, vol. 3, John Wiley & Sons, New York, 2005.
[8] M.O. Saar, Review: geothermal heat as a tracer of large-scale groundwater flow and as a means to determine permeability fields, Hydrogeol. J. 19 (1) (2011) 31–52.
[9] A.L. Snijders, G.J. Groenveld, J. Vermeer, G.M.L.M. van de Wiel, Moisture migration and drying-out in sand around heat dissipating cables and ducts, A theoretical and experimental study, company report, KEMA (1981).
[10] O.E. Gouda, A.Z. El Dein, G.M. Amer, Effect of the formation of the dry zone around underground power cables on their ratings, IEEE Trans. Power Deliv. 26 (2) (2011) 972–978.
[11] R. de Lieto Vollaro, L. Fontana, A. Vallati, Experimental study of thermal field deriving from an underground electrical power cable buried in non-homogeneous soils, Appl. Therm. Eng. 62 (2) (2014) 390–397.
[12] T.L. Brandon, J.K. Mitchell, J.T. Cameron, Thermal instability in buried cable backfills, J. Geotech. Eng. 115 (1) (1989) 38–55.
[13] S. Ahmad, et al., Evolution of temperature field around underground power cable for static and cyclic heating, Energies 14 (23) (2021) 8191.
[14] P. Ocłoń, et al., Experimental validation of a heat transfer model in underground power cable systems, Energies 13 (7) (2020) 1747.
[15] O.E. Gouda, A.Z.E. Dein, Improving underground power distribution capacity using artificial backfill materials, IET Gener. Transm. Distrib. 9 (2015) 2180–2187.
[16] O.E. Gouda, A.Z. El Dein, G.M. Amer, The effect of the artificial backfill materials on the ampacity of the underground cables, in: 2010 7th International Multi-Conference on Systems, Signals and Devices, *SSD-10*, 2010.
[17] O.E. Gouda, et al., Load cycling of underground distribution cables including thermal soil resistivity variation with soil temperature and moisture content, IET Gener. Transm. Distrib. 12 (18) (2018) 4125–4133.

[18] O.E.-S. Gouda, et al., Cyclic loading of underground cables including the variations of backfill soil thermal resistivity and specific heat with temperature variation, IEEE Trans. Power Deliv. 33 (6) (2018) 3122–3129.
[19] K. Werner, et al., Recharge and Discharge of Near-Surface Groundwater in Forsmark, Comparison of Classification Methods. R-07-08, Swedish Nuclear Fuel and Waste Management, 2007.
[20] G. Sandén, L. Maxe, J. Dahné, Grundvattennivåer Och Vattenförsörjning Vid Ett Förändrat Klimat [Groundwater Levels and Water Supply in a Changing Climate], SGU-rapport 2010:12: Geological Survey of Sweden, 2010.
[21] A. International, Standard Test Method for Determination of Thermal Conductivity of Soil and Soft Rock by Thermal Needle Probe Procedure, ASTM International, 2014.
[22] F. Gori, S. Corasaniti, Theoretical prediction of the soil thermal conductivity at moderately high temperatures, J. Heat Transfer-Transact. Asme 124 (6) (2002) 1001–1008.
[23] F. Gori, S. Corasaniti, New model to evaluate the effective thermal conductivity of three-phase soils, Int. Commun. Heat Mass Tran. 47 (Supplement C) (2013) 1–6.
[24] W.H. Leong, et al., Inter-particle contact heat transfer model: an extension to soils at elevated temperatures, Int. J. Energy Res. 29 (2) (2005) 131–144.
[25] J.R. Philip, D.A. De Vries, Moisture movement in porous materials under temperature gradients, Trans. Am. Geophys. Union 38 (2) (1957) 222–232.
[26] I.V. Nikolaev, W.H. Leong, M.A. Rosen, Experimental investigation of soil thermal conductivity over a wide temperature range, Int. J. Thermophys. 34 (6) (2013) 1110–1129.
[27] V.R. Tarnawski, W.H. Leong, K.L. Bristow, Developing a temperature-dependent Kersten function for soil thermal conductivity, Int. J. Energy Res. 24 (15) (2000) 1335–1350.
[28] O. Johansen, Thermal Conductivity of Soils, PhD Thesis, Institute for Kjoleteknikk, Trondheim, Norway, 1975. Cold Regions Research and Engineering Lab Hanover NH, 1977.
[29] M.S. Kersten, Thermal Properties of Soils, Institute of technology: University of Minnesota, 1949.